RSC Advances

PAPER

View Article Online
View Journal | View Issue

Cite this: *RSC Adv.*, 2015, **5**, 81808

9-*N*-Alkylaminomethylanthracene probes for selective fluorescence sensing of pentafluorophenol†

Anup Pandith, Ashwani Kumar and Hong-Seok Kim*

Received 8th August 2015
Accepted 18th September 2015

DOI: 10.1039/c5ra15900h

www.rsc.org/advances

9-*N*-Alkylaminomethylanthracenes (**1** and **2**) were synthesised for halophenol sensing, and their selectivity and sensitivity towards pentafluorophenol (PFP) in ethanol were investigated. Probe **1** exhibited a good selectivity and sensitivity for PFP with a high association constant (4.35×10^5 M^{-1}) without any interference from other halophenols. The relatively high selectivity and sensitivity of probe **1** are caused by strong intermolecular hydrogen bonding interactions. The interaction of PFP with probes **1** and **2** was analysed through UV-Vis, fluorescence, and ^{1}H NMR spectroscopy, and was further supported by DFT calculations. The limit of detection for PFP was 2 μM in ethanol using probe **1**.

1. Introduction

Among the various phenol derivatives, mono-,[1] di-,[2] tri-,[3] tetra-,[4] and pentahalophenols are anthropogenic environmental pollutants. Most halophenol derivatives, especially fluorophenols, are used as agrochemicals such as herbicides,[5] insecticides,[6] and fungicides,[7] and are also vital precursors for the synthesis of various pharmaceutically important compounds such as amino acids,[8] peptides,[9] and nucleosides. Additionally, some derivatives are also used in the synthesis of antitumor agents and HIV inhibitors.[10] Thus, large amounts of fluorophenolic compounds are released into the environment. Unlike mono-, di-, and trihalophenols, tetra- and pentahalophenols cannot be degraded by aerobic or anaerobic microbial species under ordinary conditions.[11] The stability of xenobiotic pentafluorophenol (PFP) and its derivatives is attributable to its electron-deficient benzene ring, which contains a highly electronegative fluorine atom. The stability of the carbon–fluorine bond is 116 kcal mol^{-1} in CH_3F, whereas that of the carbon–chlorine bond is 81 kcal mol^{-1} in CH_3Cl.[12] The high electronegativity of fluorine causes strong polarisation of the C–F bond in fluoro-organic compounds that facilitates easy dissociation in water such as lakes and rivers by inducing hydrophilic properties.[13] Thus, the accumulation of PFP in environments may cause dangerous chronic diseases in humans and animals because of its bio-hazardous properties.[14] Despite its known effects, PFP is being increasingly applied, thus increasing the release of this compound into the environment, which can cause problems in the future. Recently, several attempts have been made to detect the most hazardous halophenols in the environment using chromatography, electrochemical methods,[15] adsorption on granular activated carbon materials,[16] ^{19}F NMR,[17] fibre optics,[18] and biochemical and electro-chromic techniques.[19] Simple and small molecular architectures have attracted great interest in the supramolecular chemistry field because of their fast and straight forward synthesis and the possibility of controlling their solubility by altering their chemical functionalisation and structure. Nitrogen-containing pyridine- and imidazole-appended probes have been utilised to detect various neutral molecules such as carboxylic acids,[20] amides,[21] and amino acids.[22] To the best of our knowledge, anthracene-based fluorescent probes with potential binding sites of secondary amines and imidazole have not been previously reported for the detection of fluorophenol derivatives.

In the present work, we synthesised 9-*N*-alkylaminomethylanthracene based probes **1** and **2** for the detection of halo phenols. Probe **1** exhibited selective and sensitive "*switch on*" blue fluorescence emission with PFP among the different phenol derivatives whereas probe **2** was synthesised as a model compound for comparison. The binding behaviour of probes **1** and **2** towards PFP was studied by using UV-Vis, fluorescence, ^{1}H NMR studies and further supported by DFT calculations (Fig. 1).

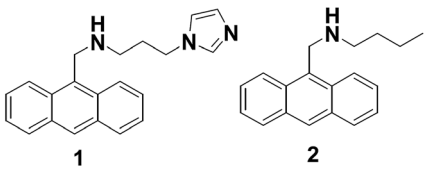

1 2

Fig. 1 Structures of 9-*N*-alkylaminomethylanthracene probes **1** and **2**.

Department of Applied Chemistry, School of Applied Chemical Engineering, Kyungpook National University, Daegu 702-701, Republic of Korea. E-mail: kimhs@knu.ac.kr; Fax: +82 53 9506594; Tel: +82 53 9505588

† Electronic supplementary information (ESI) available. See DOI: 10.1039/c5ra15900h

2. Results and discussion

Recently, we reported using a 1-(3-imidazolepropyl)aminomethylpyrene probe to detect salicylic acid derivatives through an '*off–on*' response.[23] Building on this concept, we applied a simple anthracene fluorophore to detect neutral molecules by observing the variation of its blue fluorescence emission upon binding various halophenol derivatives. Probes **1** and **2** were prepared by a $TiCl(O^iPr)_3$-mediated reductive amination of 9-anthracenecarboxaldehyde with 1-(3-aminopropyl)imidazole or *n*-butylamine in the presence of $NaBH(OAc)_3$ in good yields (Scheme 1). The ^1H NMR spectrum of probe **1** in DMSO-d_6 showed an AnCH_2NH proton at δ 4.59 as a singlet and ImH-5 and H-4 protons at δ 6.83 and δ 7.06, respectively. In the ^{13}C NMR spectrum of **1** imidazole, C-2 appeared at δ 137.15 and AnCH_2NH was observed at δ 46.85. The high-resolution mass spectrum (HRMS) of **1** clearly showed a molecular ion peak for $[M + H]^+$ at *m*/*z* 316.1813 (see ESI†). Similarly, probe **2** also exhibited characteristic peaks in ^1H and ^{13}C NMR spectra, as well as a HRMS peak at *m*/*z* 264.1689. All spectral features supported the successful synthesis of probes **1** and **2**.

The UV-Vis absorption spectrum of probe **1** (20 μM) in EtOH exhibited typical anthracene absorption maxima at λ_{max} = 331, 348, 365, and 385 nm (Fig. 2). The absorption bands of probe **1** were mostly due to n–π* and π–π* transitions. Upon the addition of various halophenols such as pentafluorophenol (PFP), 2,3,5,6-tetrafluorophenol (TFP), 2,4,6-trichlorophenol (TCP), 2,4-difluorophenol (2,4-DFP), 2-fluorophenol (2-FP), 4-chlorophenol (4-CP), 4-bromophenol (4-BP), 4-iodophenol (4-IP), and phenol (P), only PFP exhibited a significant change in the absorption maxima at λ_{max} = 331 and 348 nm. The molar absorptivity (log ε) of probe **1** at λ_{max} = 331 and 348 nm were changed from 3.40 and 3.34 to 3.94 and 3.10 M^{-1} cm^{-1}, respectively. Other halophenols did not show any obvious changes in the UV-Vis spectra of probe **1** (Fig. 2). The substantial changes in the spectra of probe **1** after the addition of PFP were suggestive of significant interactions between probe **1** and the electron-deficient PFP.

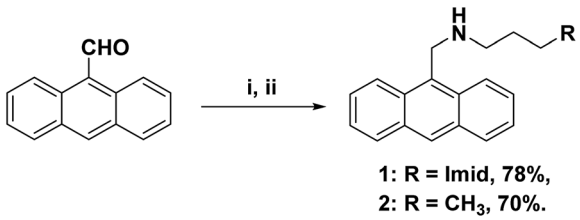

Scheme 1 Synthesis of 9-*N*-alkylaminomethylanthracene probes **1** and **2**. Reaction conditions (i) R–NH_2, $TiCl(O^iPr)_3$, CH_2Cl_2, rt, 16 h; (ii) $NaBH(OAc)_3$, 2 h.

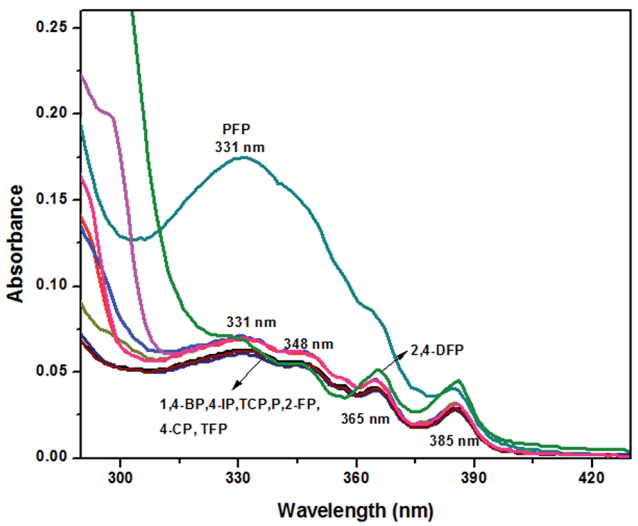

Fig. 2 UV-Vis spectra of probe **1** (20 μM) in the presence of various halophenol derivatives (10 eq. each) in EtOH.

The fluorescence emission spectrum of probe **1** (20 μM) in EtOH revealed characteristic peaks at λ_{em} = 395, 417, and 443 nm upon excitation at 365 nm (Fig. 3). Various solvents such as dimethylsulfoxide (DMSO), acetonitrile, isopropylalcohol, and methanol were studied to evaluate the fluorescence emission behaviour. Ethanol showed the best result for the selective sensing of PFP (Fig. S1†).

Probe **1** exhibited relatively very low fluorescence emission ('*off*' mode) with a very low quantum yield (Φ_1 = 0.0019). In order to verify the emission behaviour at other absorption peaks such as 331, 348 and 385 nm, probe **1** was also excited using these and the fluorescence studies showed that the emission intensity found to be the best with 365 nm than any other (331, 348 and 385 nm) (Fig. S2†) and it was standardised for further fluorescence experiments. Upon the addition of PFP (10 eq.) to probe **1**, the fluorescence emission was enhanced by nearly 10 times (Φ_{1+PFP} = 0.0891), additionally, TFP caused minor fluorescence enhancement (Φ_{1+TFP} = 0.0305) and other halophenols, including TCP, 2,4-DFP, 4-CP, 4-BP, 4-IP, and P, did not exert any effect on fluorescence emission (Fig. 3). Other than halophenols, fluorescence studies also performed with the miscellaneous phenol derivatives including 2-aminophenol (2-AP), 4-cyanophenol (4-CNP), 4-nitrophenol (4-NP), 1,2,3-trihydroxybenzene (THB), 2,4-dinitrophenol (DNP), thiophenol (TP), 2-aminothiophenol (ATP), however none of these revealed any responses (Fig. S3†).

To investigate the binding strength and stoichiometry of probe **1** with PFP, fluorescence titration and Job's plot experiments were performed in EtOH. Gradual addition of PFP to probe **1** (20 μM) caused a gradual increase in the emission intensity at λ_{em} = 395, 417, and 443 nm, and saturation was achieved after 1.0 eq. of PFP was added. The fitting of the fluorescence titration data at λ_{em} = 417 nm revealed the formation of a 1 : 1 complex with a good association constant: $K_a = 4.35 \times 10^5$ M^{-1} (±6.50%) (Fig. 4a). In a Job's plot experiment, the maximum fluorescence intensity was obtained when the mole fraction of PFP reached 0.5; this finding also supported the formation of a 1 : 1 complex (Fig. 4b). By plotting the polynomial relationship between the fluorescence intensity at λ_{max} = 417 nm of probe **1** and [PFP] μm, the limit of detection (LOD) was determined to be 2 μM (R^2 = 0.99487) (Fig. S4†).

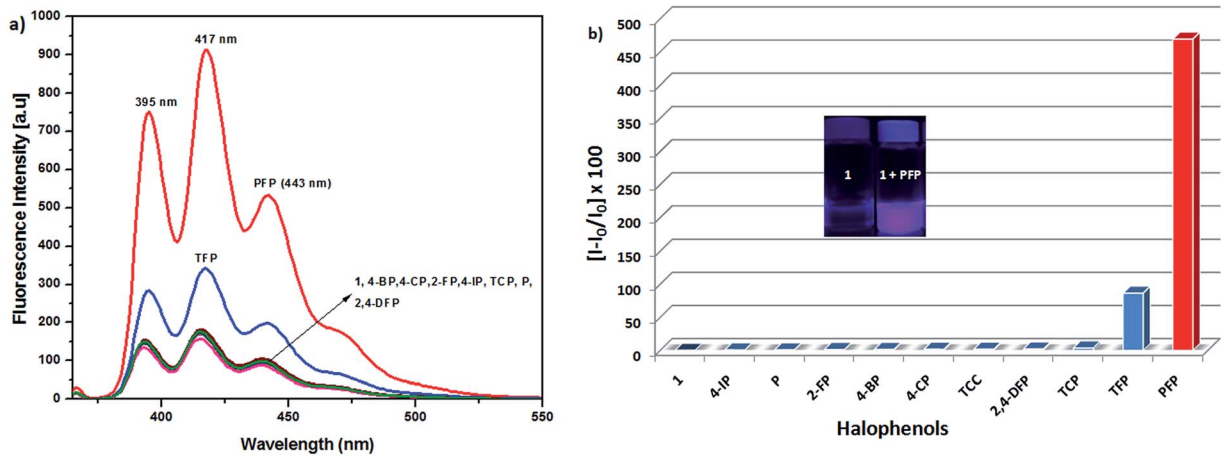

Fig. 3 (a) Fluorescence spectra of probe **1** (20 μM) in the presence of various halophenols (200 μM, each): $\lambda_{ex} = 365$ nm: (b) relative fluorescence enhancement ratio ($[I - I_0/I_0] \times 100$) intensity bar graph of probe **1** (20 μM) with various halophenols (200 μM) in EtOH: $\lambda_{ex} = 365$ nm and $\lambda_{em} = 417$ nm. The inset figure shows the fluorogenic responses of probe **1** and **1**·PFP complex.

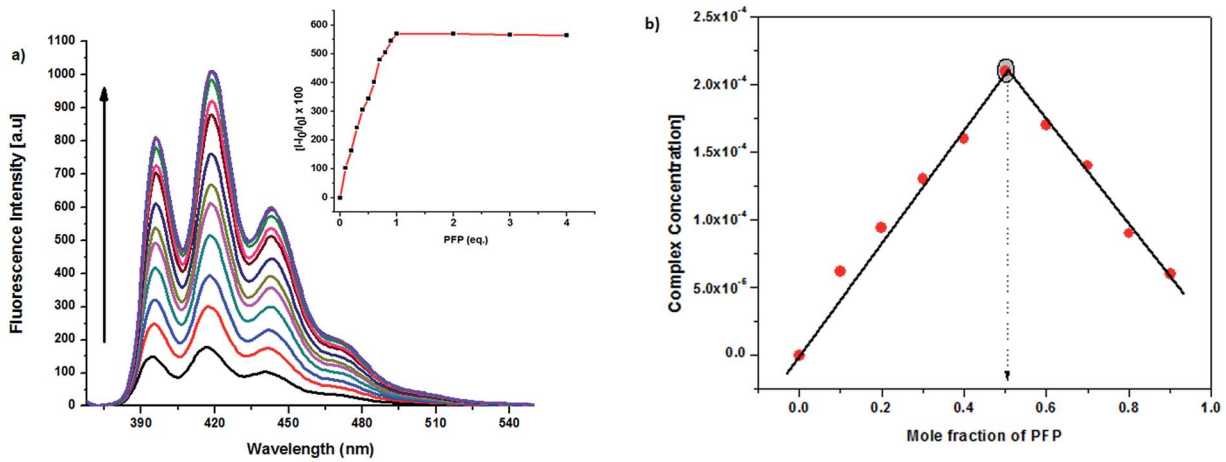

Fig. 4 (a) Fluorescence titration spectra of probe **1** (20 μM) with PFP in EtOH. The inset shows the molar ratio plots of the fluorescence enhancement: $\lambda_{ex} = 365$ nm and $\lambda_{em} = 417$ nm. (b) Job's plot of probe **1** (20 μM) with PFP (20 μM) in EtOH: $\lambda_{ex} = 365$ nm and $\lambda_{em} = 417$ nm.

UV-Vis and fluorescence studies demonstrated that probe **1** selectively binds to PFP with high selectivity compared with other halophenol derivatives. The relative fluorescence enhancement ratio $\{[I - I_0/I_0] \times 100$, where I_0 = fluorescence intensity of the probe in the absence of PFP and I = the fluorescence intensity of the probe in the presence of PFP$\}$ of probe **1** with PFP was higher than that of TFP, showing that the absence of only one fluorine atom at the *para* position caused substantially altered the fluorescence enhancement.

To improve the understanding of this behaviour, the normalised fluorescence enhancement ratio was plotted *vs.* $[(G =$ PFP/TFP$)]$, which revealed a large difference in the fluorescence enhancement ratio upon the addition of different equivalents of PFP and TFP (Fig. S5†). The effects of halogens on binding were further investigated by UV-Vis and fluorescence studies of **1** with tetrachlorocatechol (TCC) in EtOH. TCC contains four chlorine atoms and has a structure that is similar to that of PFP. However, TCC did not showed any effect on probe **1** (Fig. 3), indicating that the selectivity of the complexation with fluorinated phenol derivatives may be attributed to the existence of strong hydrogen bonding interactions between fluorophenols and the imidazole and aliphatic amine moiety of **1**. The tendency of fluorophenols to exhibit hydrogen bonding interactions with amines (the 4-fluorophenol hydrogen bonding

Table 1 Association constants K_a (M^{-1}) of probes **1** and **2** with PFP and TFP in EtOH[a]

	Association constant K_a (M^{-1})	
Halophenols	**1**	**2**
PFP	4.35×10^5	4.11×10^3
TFP	2.89×10^3	1.76×10^3

[a] Association constants were obtained from fluorescence titrations in EtOH. Errors < ±10%.

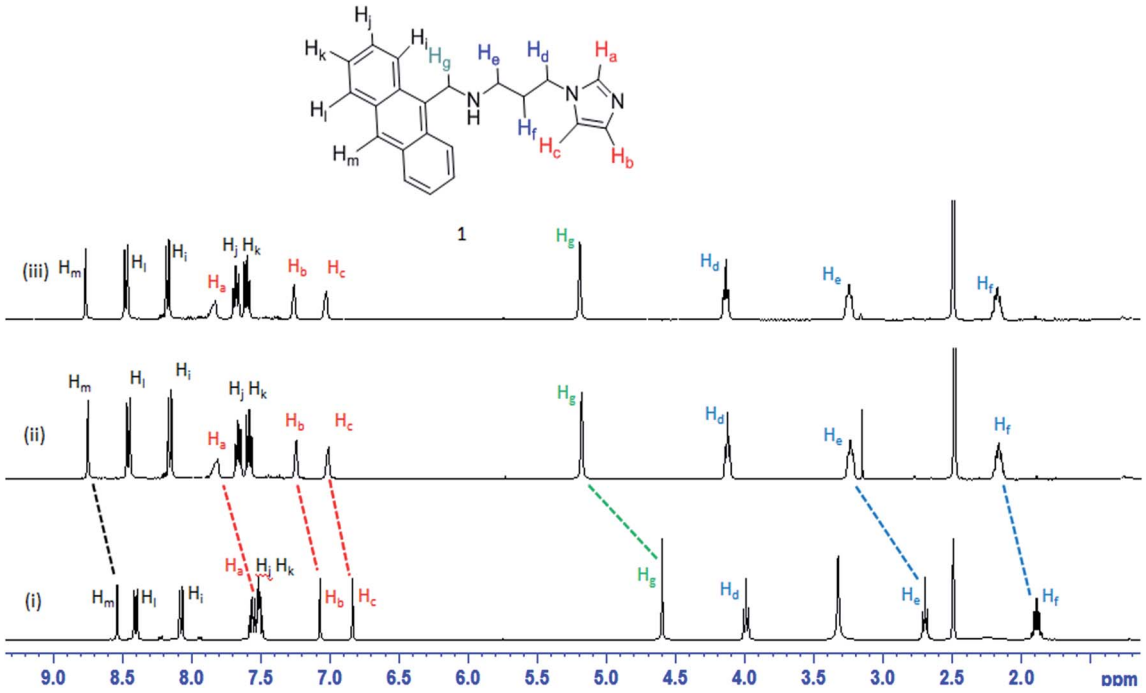

Fig. 5 Partial ^{1}H NMR spectra of (i) probe **1** (5.0×10^{-3} M), (ii) **1** + 1.0 eq. PFP, and (iii) **1** + 2.0 eq. PFP in DMSO-d_6.

affinity to amines is 40.0 kJ mol^{-1}) is higher in most of the media compared with other halophenols.[24] The relatively strong back-donation effect of the fluorine atom in most fluorophenol derivatives also contributes to stronger interactions with amines by allowing lower solvation than in other halophenols.[25] The pK_a values of PFP and TFP are 5.49 and 5.54,[26] respectively, which are very similar; this similarity suggests that the fluorescence enhancement is not solely dependent on simple protonation at the secondary amine, which inhibits the PET process, in aminoanthracene derivatives.[27] Fluorescence titration of **1** with TFP revealed the formation of a 1 : 1 complex with $K_a = 2.89 \times 10^2$ M^{-1} (±2.82%), which is 1000 times smaller than that of PFP (Fig. S6†). The fluorescence studies with halophenol derivatives at λ_{ex} = 385 nm also showed similar results (Fig. S7†).

To understand the role of the imidazole, a simple aliphatic chain was introduced in probe **2**. Probe **2** showed similar UV-Vis absorption (Fig. S8†) and fluorescence emission peaks at λ_{em} = 395, 417, and 443 nm (±2 nm) upon excitation at 365 nm with a relatively high quantum yield ($\phi_2 = 0.0032$). Interestingly, other absorption maxima such as 329 ($\phi = 0.0020$), 344 ($\phi = 0.0024$), and 385 nm ($\phi = 0.0020$) showed less fluorescence emission (Fig. S9†). Thus, the presence of the imidazole group causes only a minor quenching effect in 9-*N*-alkylaminomethylanthracene-based probes. Upon the addition of various halophenols (10 eq.), PFP and TFP showed nearly five-fold enhancements, whereas 2,4-DFP showed enhancements of one-to-two-fold at 395, 417, and 443 nm at λ_{ex} = 365 nm (Fig. S10†). The diminished selectivity observed in probe **2** could be explained by the presence of only one vital interaction site. Because of the structural similarity of PFP and TFP, these two species exhibit similar types of interactions with the secondary amine moiety being the only available limited binding site.

Based on fluorescence titration and Job's plot experiments, the association constants of PFP and TFP with probe **2** were found to be $K_a = 4.11 \times 10^3$ M^{-1} (±2.03%) and 1.76×10^3 M^{-1} (±5.41%), respectively, which are 100 times smaller than those of probe **1** (Table 1) (Fig. S11†). The Job's plot experiments of probe **2** with PFP and TFP showed the formation of a 1 : 1 complex in EtOH (Fig. S12†). The higher relative fluorescence enhancement ratio and association constant observed for probe **1** with PFP further support the importance of imidazole for the selective and sensitive recognition of PFP over other halophenols, as shown in Fig. S13.†

The fluorescence emission of the **1**·PFP complex in DMSO was weaker than that in EtOH. Additionally, no observable shift was observed in either the UV-Vis or fluorescence experiments (Fig. S14†).

To further investigate the interaction sites and mode of complexation between probe **1** and PFP, ^{1}H NMR was performed in DMSO-d_6. The addition of 1.0 eq. of PFP to a DMSO-d_6 solution of **1** led to substantial downfield shifts of two

Table 2 Proton chemical shift differences ($\Delta\delta$, in DMSO-d_6) measured for probe **1** with PFP[a]

Protons	H_a	H_b	H_c	H_d	H_e	H_f	H_g	H_m
1 (δ_1)	7.54	7.07	6.83	3.99	2.70	1.89	4.59	8.53
1 + PFP (1.0 eq.) (δ_2)	7.98	7.25	7.02	4.13	3.16	2.17	5.29	8.77
$\Delta\delta$ ($\delta_2 - \delta_1$)	0.44	0.18	0.19	0.14	0.46	0.28	0.70	0.24

[a] Chemical shift values are in ppm.

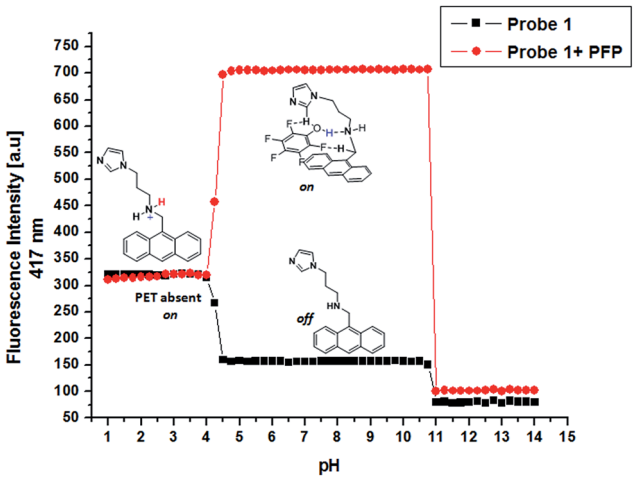

Fig. 6 The pH-dependent fluorescence studies of probe **1** (20 μM) alone and in the presence of 1.0 eq. of PFP (20 μM) from pH 1 to 14, λ_{ex} = 365 nm and λ_{em} = 417 nm in EtOH.

methylene signals (labelled g and e in Fig. 5): H_g protons from δ 4.59 to 5.29 ppm ($\Delta\delta$, 0.70) and H_e protons from δ 2.70 to 3.16 ppm ($\Delta\delta$, 0.46), respectively. Furthermore, the H_a, H_b, and H_c protons of imidazole shifted downfield from δ 7.54 to 7.98 ppm ($\Delta\delta$, 0.44), δ 7.07 to 7.25 ppm ($\Delta\delta$, 0.18), and δ 6.83 to 7.02 ppm ($\Delta\delta$, 0.19), respectively. The anthracene H_m proton shifted from δ 8.53 to 8.77 ppm ($\Delta\delta$, 0.24), clearly indicating the existence of hydrogen bonding between probe **1** and PFP. The large changes in chemical shifts of the labelled protons confirmed that both imidazole C2–H (proton a) and the secondary amine moiety bind to PFP. For this reason, the signals ascribed to the aliphatic protons g and e are shifted more downfield than d (see Table 2). The addition of a further 1.0 eq. of PFP to this solution did not result in further shifts of the proton signals, clearly indicating that a 1 : 1 complex between probe **1** and PFP was formed (Fig. 5).

The fluorescence and ^{1}H NMR studies clearly revealed that both binding strength and fluorescence enhancement depend on the position of the fluorine atom on the phenol ring. *Ortho* (2^{nd} and 6^{th}) fluorine atoms and *para* (4^{th}) fluorine atoms facilitate binding with probe **1**. No response was observed with 2,4-DFP, and relatively low enhancement was observed with TFP, which supports the proposed hypothesis.

The possible interference resulting from other halophenol derivatives on the interaction between probe **1** and PFP was investigated. Fluorescence enhancement was retained in the presence of other halophenol derivatives. Thus, probe **1** is free from interference by other halophenol derivatives (Fig. S15†).

The pH values of the halo-substituted phenols investigated ranged from 4 to 10. The most commercially used pentachlorophenol's pK_a is 4.9, which was the lowest, followed by that of PFP (5.49).[28] The pH-dependent fluorescence studies revealed that the fluorescence emission of probe **1** was turned on under pH 4.3 because of the protonation of the secondary amine in **1** and completely quenched over pH 10.75 (Fig. 6). The phenoxide ion generated from PFP in basic media (over pH 10.75) caused the complete quenching of probe **1**, and no interactions were observed between probe **1** and PFP. Therefore, probe **1** can be effectively used to detect PFP in the pH range 4–11 in EtOH.

To understand the nature of the binding mode and the complexation mechanism of PFP with probes **1** and **2**, energy-minimisation calculations using the B3LYP/6-31G* level theory for vacuum and for ethanol solvent (SM8 solvent model) were performed with Spartan 10 software. As predicted from the ^{1}H NMR studies, the energy-minimised structure (Fig. 7) also

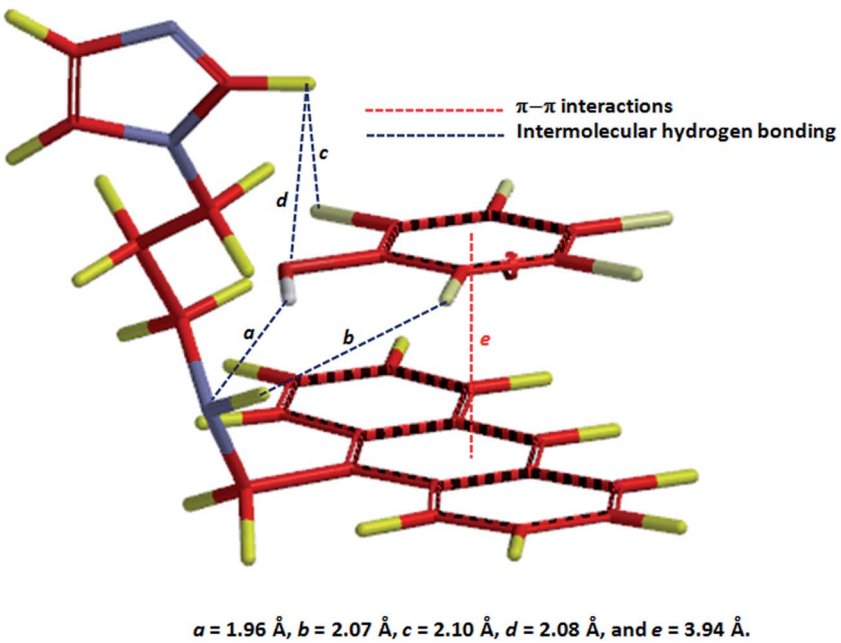

Fig. 7 Energy-minimised structure of **1**·PFP using B3LYP/6-31G* method in EtOH (implicit) medium.

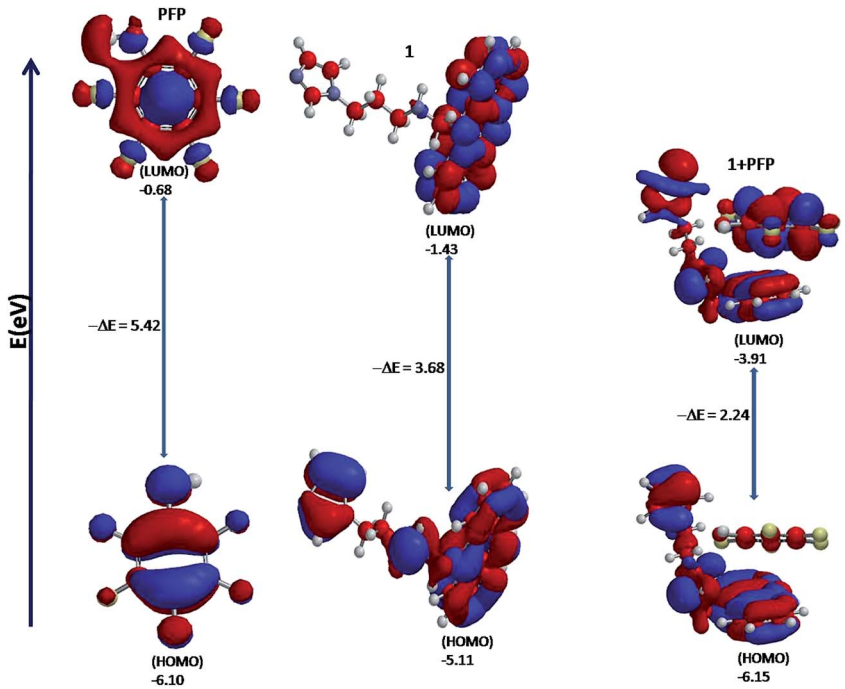

Fig. 8 HOMO and LUMO of PFP, probe **1** and **1**·PFP complex calculated by the B3LYP/6-31G* method in EtOH medium.

supported the synergic multiple hydrogen bonding and π–π interactions of the **1**·PFP complex in EtOH as an implicit solvent. In order to make more clear visualization only vital hydrogen bonding interactions are mentioned in the Fig. 7.

The energies of the highest occupied molecular orbital (HOMO) and the lowest unoccupied molecular orbital (LUMO) of probe **1** were −5.11 eV and −1.43 eV, respectively, while those of the newly formed complex **1**·PFP were −6.15 eV and −3.91 eV, respectively, indicating that the formed complex ($-\Delta E_1$ = 3.68 eV, $-\Delta E_{\mathbf{1}\cdot\mathrm{PFP}}$ = 2.24 eV) was stable (Fig. 8). The band gap energy ($-\Delta E_{\mathbf{1}\cdot\mathrm{PFP}}$ = 2.24 eV) is much smaller than ($-\Delta E_{\mathbf{2}\cdot\mathrm{PFP}}$ = 3.14 eV), which further confirms that complex stabilisation is more feasible in probe **1** than in probe **2** and similar type of binding mode observed in probe **2** with PFP and TFP further supported the UV-Vis and fluorescence results (Fig. S16†). The interaction energies of **1**·PFP and **2**·PFP were −28.82 kcal mol^{-1} and −10.21 kcal mol^{-1}, respectively, which showed that complexation is thermodynamically feasible.[29] The decreased HOMO–LUMO band gap energies of respective probes and their complexes in EtOH compared to vacuum showed the solvent effect (Table 3).[30] The optimised, most stable geometry of the **1**·PFP complex were due to the free rotation of the propyl spacer and secondary amine; additionally, imidazole facilitates stronger hydrogen bonding interactions. Similar interactions were observed for probe **2** with both PFP and TFP, supporting the UV-Vis and fluorescence results.

The higher selectivity and sensitivity observed for probe **1** toward PFP among the various halophenol derivatives could be due to the existence of strong hydrogen bonding interactions between the electronegative fluorine atoms of PFP and probe **1** (involving imidazole and the secondary amine moiety). These strong interactions occurred through the close proximity of the phenolic –OH proton of PFP to the lone pair electron of the secondary amine. In probe **1**, the PET efficiency and fluorescence emission are primarily dependent on the protonation strength and synergic interactions such as hydrogen bonding, columbic interactions, and π–π interactions. As a result, even in acidic medium (buffer-maintained pH), the inhibition of PET is not very strong, whereas in the presence of PFP, PET inhibition is relatively effective. The additional effect of imidazole on the suppression of fluorescence in ethanol is also altered by the hydrogen bonding interactions with PFP in EtOH. Although the observed hydrogen bonding distance between the H_m proton (10th position on the anthracene moiety) and the *para* fluorine is larger, it should not be ignored because of the π–π interactions between the highly electron-rich and electron-deficient rings of the probe and PFP, which contribute to increase the probe's selectivity for PFP over TFP.

Table 3 Calculated band gap energies (eV) and interaction energies (kcal mol^{-1}) of probes **1** and **2** with their complexes with PFP[a]

	Band gap energy ($-\Delta E$, eV)		Interaction energy (kcal mol^{-1})	
Probe	$-\Delta E_{vac}$	$-\Delta E_{EtOH}$	$-\Delta E_{vac}$	$-\Delta E_{EtOH}$
Probe **1**	2.41	2.24	93.00	28.82
Probe **2**	4.27	3.14	42.00	10.21

[a] HOMO–LUMO band gap energies (eV) and interaction energies (kcal mol^{-1}) were calculated through the B3LYP/6-31G* method.

3. Conclusion

In conclusion, the simple 9-*N*-(3-imidazolylpropylamino)methylanthracene probe **1** was prepared and investigated using UV-Vis, fluorescence, and ^{1}H NMR spectroscopic methods. Probe **1** selectively recognised the xenobiotic PFP over the other selected halophenols with a high association constant (4.35×10^5 M^{-1}) in EtOH and showed a very low detection limit (2 μM) due to the presence of flexible propyl spacer between imidazole N and secondary amine for optimised geometry with PFP through synergic multiple interactions *i.e.* hydrogen bonding; and π–π interactions, which resulted in an '*off–on*' mode of response. The binding phenomenon was monitored by UV-Vis and fluorescence experiments to observe enhancement effects and ^{1}H NMR to observe shifts; these studies were supported by DFT-based computational studies.

4. Experimental section

4.1 General

The melting points were determined using a Thomas-Hoover capillary melting point apparatus and were uncorrected. ^{1}H and ^{13}C NMR spectra were recorded on a Bruker AM-400 spectrometer. FAB mass spectra were collected at the KBSI Daegu branch. UV-Vis, absorption spectra were recorded on a Shimadzu UV-1650PC spectrophotometer. Fluorescence spectra were measured on a Shimadzu RF-5301 fluorescence spectrometer equipped with a xenon discharge lamp using 1 cm quartz cells with slit 3. All measurements were performed at 298 K. Analytical-grade ethanol was purchased from Merck. 1-(3-Aminopropyl)imidazole and other compounds used for the synthesis were purchased from Aldrich Chemical Co. and were used as received. Fluorescence quantum yields were determined by integration of the corrected fluorescence spectra. Quinine hemisulfate in 0.5 mol L^{-1} H_2SO_4 was used to correct fluorescence spectra as a fluorescent standard ($\Phi = 0.54$).[31]

4.2 Association constant calculations

The association constants of probes **1** and **2** were calculated using Gnuplot *ver.* 4 software with the reduced chi-square method (error bound ± 10.0%) and the curve-fitting method (error bound ± 5.0%) from the adjusted r-square method using fluorescence titration data. Solutions (20.0×10^{-6} M) of probes **1** and **2** were prepared in 50 mL volumetric flasks (±0.025 mL) (see ESI†).

4.3 Theoretical calculations

Theoretical calculations were carried out according to the literature.[32]

4.4 Synthesis of probes

Synthesis of probe 1. A mixture of 9-anthracenecarboxaldehyde (50 mg, 0.24 mmol), 1-(3-aminopropyl)imidazole (36 mg, 0.29 mmol), and $TiCl(O^iPr)_3$ (0.37 mL, 0.29 mmol) in CH_2Cl_2 (8 mL) was stirred at room temperature for 12 h, and then, $NaBH(OAc)_3$ (61 mg, 0.29 mmol) was added. The resulting mixture was stirred for an additional 2 h. After the reaction was completed, the solvent was removed. The residue was neutralised with $NaHCO_3$ solution and extracted with ethyl acetate. The organic layer was dried over anhydrous Na_2SO_4 and concentrated to dryness. The residue was purified by silica gel chromatography (elution with 10% MeOH in CH_2Cl_2, $R_f = 0.7$) to give **1** in 78% yield (58 mg). Mp 109–110 °C; ^{1}H NMR (400 MHz, DMSO-d_6) δ 1.88 (m, 2H, H_f), 2.69 (t, $J = 7.1$ Hz, 2H, H_e), 3.98 (t, $J = 6.9$ Hz, 2H, H_d), 4.59 (s, 2H, H_g), 6.83 (s, 1H, H_c), 7.06 (s, 1H, H_b), 7.48–7.57 (m, 5H, $H_{j,k}$–Ant, Im–H_a), 8.07 (d, $J = 8.1$ Hz, 2H, H_i–Ant), 8.39 (d, $J = 7.9$ Hz, 2H, H_l–Ant), 8.88 (s, 1H, H_m–Ant); ^{13}C NMR (100 MHz, DMSO-d_6) δ 30.9, 44.0, 45.1, 46.4, 119.3, 124.8, 125.0, 125.8, 126.6, 128.2, 128.8, 129.9, 131.0, 132.2, 137.2; HR mass $C_{21}H_{21}N_3$ $[M + H]^+$: 316.1814, found: *m*/*z* 316.1813.

Synthesis of probe 2. A mixture of 9-anthracenecarboxaldehyde (50 mg, 0.24 mmol), *n*-butylamine (21 mg, 0.29 mmol), and $TiCl(O^iPr)_3$ (0.37 mL, 0.29 mmol) in CH_2Cl_2 (8 mL) was stirred at room temperature for 12 h, and then, $NaBH(OAc)_3$ (61 mg, 0.29 mmol) was added. Work up was performed as described for probe **1**. The residue was purified by silica gel column chromatography (elution with 2% MeOH in CH_2Cl_2, $R_f = 0.5$) to give **2** in 70% yield (45 mg) as a gummy solid. ^{1}H NMR (400 MHz, DMSO-d_6) δ 0.87 (t, $J = 7.0$ Hz, 3H, $NHCH_2CH_2$-CH_2CH_3), 1.32 (m, 2H, $NHCH_2CH_2CH_2$), 1.47 (m, 2H, $NHCH_2$-CH_2), 2.76 (t, $J = 6.9$ Hz, 2H, $NHCH_2$), 4.62 (s, 2H, CH_2NH), 7.49–7.58 (m, 4H, $H_{j,k}$–Ant), 8.07 (d, $J = 8.1$ Hz, 2H, H_i–Ant), 8.40 (d, $J = 7.9$ Hz, 2H, H_l–Ant), 8.53 (s, 1H, H_m–Ant); ^{13}C NMR (100 MHz, DMSO-d_6) δ 13.9, 20.0, 31.5, 45.2, 49.5, 124.7, 125.0, 125.8, 126.5, 126.8, 128.8, 129.9, 131.0, 132.2, 134.6; HR mass $C_{19}H_{21}N$ $[M + H]^+$: 264.1688, found: *m*/*z* 264.1689.

Acknowledgements

This research was supported by the Basic Science Research Program through the National Research Foundation of Korea (NRF) funded by the Ministry of Science, ICT, Future Planning, Republic of Korea (2013R1A1A2006777) and BK21 plus program.

References

1 (*a*) M. Cao, L. Wang, Z. Ai and L. Zhang, *J. Hazard. Mater.*, 2015, **292**, 27–33; (*b*) B. D. Key, R. D. Howell and C. S. Criddle, *Environ. Sci. Technol.*, 1997, **31**, 2445–2454; (*c*) M. M. Häggblom and L. Y. Young, *Appl. Environ. Microbiol.*, 1995, **61**, 1546–1550; (*d*) R. L. Osborne, G. M. Raner, L. P. Hager and J. H. Dawson, *J. Am. Chem. Soc.*, 2006, **128**, 1036–1037.

2 (*a*) S. J. Tavener and J. H. Clark, *J. Fluorine Chem.*, 2003, **123**, 31–36; (*b*) M. M. Häggblom, *FEMS Microbiol. Rev.*, 1992, **9**, 29–71; (*c*) M. G. Boersma, I. P. Solyanikova, W. J. V. Berkel, J. Vervoort, L. A. Golovleva and I. M. Rietjens, *J. Ind. Microbiol. Biotechnol.*, 2001, **26**, 22–34.

3 (*a*) J. W. Yager, D. A. Eastmond, M. L. Robertson, W. M. Paradisin and M. T. Smith, *Cancer Res.*, 1990, **50**, 393–399; (*b*) B. Key, R. Howell and C. Criddle, *Environ. Sci.*

Technol., 1997, **31**, 2445–2454; (*c*) A. M. Osman, S. Boern, M. G. Boersma, C. Veeger and I. M. Rietjens, *Proc. Natl. Acad. Sci. U. S. A.*, 1997, **94**, 4295–4299.

4 (*a*) G. M. Brooke, *J. Fluorine Chem.*, 1997, **86**, l–76; (*b*) A. Harkey, H.-J. Kim, S. Kandagatla and G. M. Raner, *Biotechnol. Lett.*, 2012, **34**, 1725–1731; (*c*) M. Hofrichter, F. Bublitz and W. Fritsche, *J. Basic Microbiol.*, 1994, **34**, 163–172.

5 (*a*) A. F. Duque, V. S. Bessa and P. M. L. Castro, *J. Ind. Microbiol. Biotechnol.*, 2104, **41**, 97–104; (*b*) R. Blasco, R.-M. Wittich, M. Mallavarapu, K. N. Timmis and D. H. Pieper, *J. Biol. Chem.*, 1995, **270**, 29229–29235; (*c*) A. F. Duque, V. S. Bessa, M. F. Carvalho and P. M. L. Castro, *Bioresour. Technol.*, 2011, **102**, 9300–9303; (*d*) T. Fujiwara and D. O'Hagan, *J. Fluorine Chem.*, 2014, **167**, 16–29.

6 (*a*) V. E. Boyko, A. A. Tyutyunov, V. L. Don and S. M. Igoumnov, *Fluorine Notes*, 2013, **6**, 2013–2017; (*b*) C. D. Murphy, *J. Integr. Biol.*, 2007, **11**, 314–324; (*c*) C. Vargas, B. Song, M. Camps and M. M. HaÈggblom, *Appl. Microbiol. Biotechnol.*, 2000, **53**, 342–347.

7 (*a*) R. Natarajan, R. Azerad, B. Badet and E. Copin, *J. Fluorine Chem.*, 2005, **126**, 424–435; (*b*) G. S. Cooper and S. Jones, *Environ. Health Perspect.*, 2008, **116**, 1001–1008.

8 (*a*) B. Boutevin, A. Rousseau and D. Bosc, *J. Polym. Sci., Part A: Polym. Chem.*, 1992, **30**, 1279–1286; (*b*) J. Yu, P. Otten, Z. Ma, W. Cui, L. Liu and R. P. Mason, *Bioconjugate Chem.*, 2004, **15**, 1334–1341.

9 (*a*) A. R. Franco, A. C. Ferreira and P. M. L. Castro, *Chemosphere*, 2014, **111**, 260–265; (*b*) R. G. Pews and J. A. Gall, *J. Fluorine Chem.*, 1990, **50**, 377–380.

10 (*a*) V. S. Bondar, M. G. Boersma, E. L. Golovlev, J. Vervoort, W. J. H. van Berkel, Z. I. Finkelstein, I. P. Solyanikova, L. A. Golovleva and I. M. C. M. Rietjens, *Biodegradation*, 1998, **9**, 475–486; (*b*) H. Nemoto, T. Nishiyama and S. Akai, *Org. Lett.*, 2011, **13**, 2714–2717.

11 (*a*) E. Schmidt and H.-J. Knackmuss, *Biochem. J.*, 1980, **192**, 339–347; (*b*) K. Selvam, M. Muruganandham, I. Muthuvel and M. Swaminathan, *Chem. Eng. J.*, 2007, **128**, 51–57; (*c*) C. D. Murphy, *Biotechnol. Lett.*, 2010, **32**, 351–359; (*d*) A. F. Duque, V. S. Bessa, M. F. Carvalho, M. K. de Kreuk, M. C. M. van-Loosdrecht and P. M. L. Castro, *Water Res.*, 2011, **45**, 6745–6752; (*e*) R. Barbara, S. Genthner, G. T. Townsend and P. J. Chapman, *Biodegradation*, 1990, **1**, 65–74; (*f*) U. M. Reinscheid, M. P. Bauer and R. Miiller, *Biodegradation*, 1996, **7**, 455–461.

12 (*a*) K. H. van Pée and S. Unversucht, *Chemosphere*, 2003, **52**, 299–312; (*b*) G. R. Chaudhry and S. Chapalamadugu, *Microbiol. Mol. Biol. Rev.*, 1991, **55**, 59–79.

13 E. J. Kim, J. R. Jeon, Y. M. Kim, K. Murugesan and Y. S. Chang, *Appl. Microbiol. Biotechnol.*, 2010, **87**, 1569–1577.

14 A. M. Osman, M. A. Posthumus, C. Veeger, P. J. V. Bladeren, C. Laane and I. M. Rietjens, *Chem. Res. Toxicol.*, 1998, **11**, 1319–1325.

15 (*a*) C. Cui, X. Quan, S. Chen and H. Zhao, *Sep. Purif. Technol.*, 2005, **47**, 73–79; (*b*) I. McLellan, A. Hursthouse, C. Morrison, A. Varela and C. S. Pereira, *Environ. Monit. Assess.*, 2014, **186**, 1281–1293; (*c*) H. Jiang, D. Zhang and R. Wang, *Nanotechnology*, 2009, **20**, 145501–145508; (*d*) C.-S. Prado, G. G. Murcott, F. Marken, J. S. Foord and R. G. Compton, *Electroanalysis*, 2002, **14**, 975–979; (*e*) N. Fattahi, Y. Assadi, M. R. M. Hosseini and E. Z. Jahromi, *J. Chromatogr. A*, 2007, **1157**, 23–29.

16 (*a*) S. Azizian, Z. Niknam and E. Rombi, *J. Dispersion Sci. Technol.*, 2012, **33**, 206–212; (*b*) D. Li, D. Zeng, J. Huang, J. Gong, P. Yan, S. Ge, W. Peng, L. Ding and Y. Yuan, *IEEE Sens. J.*, 2014, **14**, 3693–3699; (*c*) N. S. Kumar, M. Suguna, M. V. Subbaiah, A. S. Reddy, N. P. Kumar and A. Krishnaiah, *Ind. Eng. Chem. Res.*, 2010, **49**, 9238–9247.

17 (*a*) R. Solná, S. Sapelnikova, P. Skládal, M. W. Nielsen, C. Carlsson, J. Emnéus and T. Ruzgas, *Talanta*, 2005, **65**, 349–357; (*b*) C. Pizarro, C.-S. González, N. P.-D. Notario and J. M.-G. Sáiz, *J. Chromatogr. A*, 2010, **1217**, 7630–7637.

18 (*a*) K. Kipper, K. Herodes and I. Leito, *J. Chromatogr. A*, 2011, **1218**, 8175–8180; (*b*) M. C. Ramos, M. C. Torijas and A. N. DõÂaz, *Sens. Actuators, B*, 2001, **73**, 71–75; (*c*) V. Thatshanamoorthy and V. Narayanan, *Asian J. Chem.*, 2013, **25**, 6083–6086; (*d*) M. P. Xavier, B. Vallejo, M. D. Marazuela, M. C.-M. Bondi, F. Baldini and A. Falai, *Biosens. Bioelectron.*, 2000, **14**, 895–905.

19 (*a*) T. Basovaa, V. Plyashkevicha, A. Hassanb, A. G. Gürekc, G. Gümüs and V. Ahsenc, *Sens. Actuators, B*, 2009, **139**, 557–562; (*b*) P. Ncube, R. W. Krause and B. B. Mamba, *Sensors*, 2011, **11**, 4598–4608; (*c*) H. X. Liu and G. H. Zhao, *Appl. Mech. Mater.*, 2013, **295–298**, 95–99; (*d*) J. Zolgharnein, T. Shariatmanesh and A. Babaei, *Sens. Actuators, B*, 2013, **186**, 536–544.

20 (*a*) S. Goswami, K. Ghosh and S. Dasgupta, *J. Org. Chem.*, 2000, **65**, 1907–1914; (*b*) S. Goswami, K. Ghosh and R. Mukherjee, *Tetrahedron*, 2001, **57**, 4987–4993; (*c*) T. Moriuchi, K. Yoshida and T. Hirao, *Org. Lett.*, 2003, **5**, 4285–4288; (*d*) P. Molina, A. Tárraga and F. Otón, *Org. Biomol. Chem.*, 2012, **10**, 1711–1724.

21 (*a*) J. Yoon, J. R. Jadhav, J. M. Kim, M. Cheong, H.-S. Kim and J. Kim, *Chem. Commun.*, 2014, **50**, 7670–7672; (*b*) S. Goswami, K. Ghosh and S. Dasgupta, *J. Org. Chem.*, 2000, **65**, 1907–1914; (*c*) T. Moriuchi, K. Yoshida and V. Hirao, *Org. Lett.*, 2013, **5**, 4285–4288.

22 (*a*) J. R. Jadhav, M. W. Ahmad and H.-S. Kim, *Tetrahedron Lett.*, 2010, **51**, 5954–5958; (*b*) J. Yoon, S. K. Kim, N. T. Singh and K. S. Kim, *Chem. Soc. Rev.*, 2006, **35**, 355–360; (*c*) Y. R. Yi, K.-S. Kim, A. Helal and H.-S. Kim, *Supramol. Chem.*, 2012, **25**, 16–23; (*d*) K. Ghosh and A. R. Sarkar, *Tetrahedron Lett.*, 2009, **50**, 85–88.

23 M. W. Ahmad, B.-Y. Kim and H.-S. Kim, *New J. Chem.*, 2014, **38**, 1711–1716.

24 (*a*) C. Laurence, J. Graton, M. Berthelot, F. Besseau, J.-Y. le Questel, M. Lucon, C. Ouvrard, A. Planchat and E. Renault, *J. Org. Chem.*, 2010, **75**, 4105–4123; (*b*) C. Gasbarri and G. Angelini, *RSC Adv.*, 2014, **4**, 17840–17845.

25 (*a*) E. J. Forbers, R. D. Richardson, M. Stacey and J. C. Tatlow, *J. Chem. Soc.*, 1959, **404**, 2019–2020; (*b*) I. V. Korendovych, M. Cho, O. V. Makhlynets, P. L. Butler, R. J. Staples and E. V. R. Akimova, *J. Org. Chem.*, 2008, **73**, 4771–4782.

26 K. Kipper, K. Herodes and I. Leito, *J. Chromatogr. A*, 2011, **1218**, 8175–8180.
27 A. P. de-Silva, T. S. Moody and G. D. Wrighta, *Analyst*, 2009, **134**, 2385–2393.
28 A. Kruve, K. Kaupmees, J. Ligand and I. Leito, *Anal. Chem.*, 2014, **86**, 4822–4830.
29 (*a*) A. Kumar, M. K. Ghosh, C.-H. Choi and H.-S. Kim, *RSC Adv.*, 2015, **5**, 23613–23621; (*b*) J. Pan, F. Tang, A. Ding, L. Kong, L. Yang, X. Tao, Y. Tian and J. Yang, *RSC. Adv.*, 2015, **5**, 191–195; (*c*) M. Karelson and V. S. Lobanov, *Chem. Rev.*, 1996, **96**, 1027–1043.
30 M. Targema, N. O. Obi-Egbedi and M. D. Adeoye, *Comput. Theor. Chem.*, 2013, **1012**, 47–53.
31 T. Morozumi, T. Anada and H. Nakamura, *J. Phys. Chem. B*, 2001, **105**, 2923–2931.
32 (*a*) A. Kumar and H.-S. Kim, *New J. Chem.*, 2015, **39**, 2935–2942; (*b*) A. Kumar, A. Pandith and H.-S. Kim, *Dyes Pigm.*, 2015, **122**, 351–358.